Article

Detection of Mismatched DNA on Partially Negatively Charged Diamond Surfaces by Optical and Potentiometric Methods

Shoma Kuga, Jung-Hoon Yang, Hironori Takahashi,
Kazuyuki Hirama, Takayuki Iwasaki, and Hiroshi Kawarada

J. Am. Chem. Soc., **2008**, 130 (40), 13251-13263 • DOI: 10.1021/ja710167z • Publication Date (Web): 10 September 2008

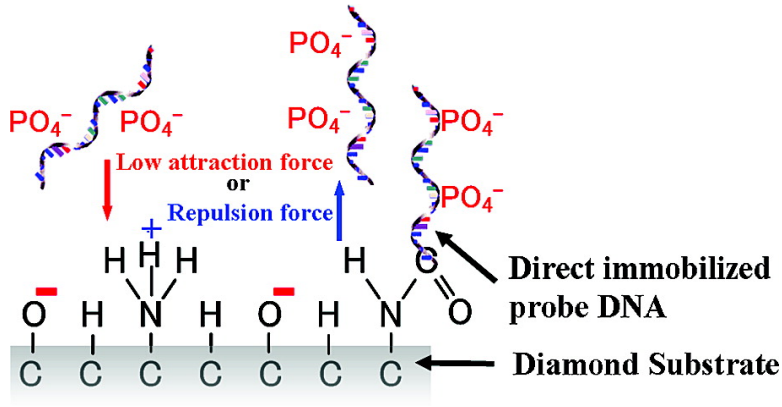

More About This Article

Additional resources and features associated with this article are available within the HTML version:

- Supporting Information
- Links to the 1 articles that cite this article, as of the time of this article download
- Access to high resolution figures
- Links to articles and content related to this article
- Copyright permission to reproduce figures and/or text from this article

View the Full Text HTML

J|A|C|S
ARTICLES

Published on Web 09/10/2008

Detection of Mismatched DNA on Partially Negatively Charged Diamond Surfaces by Optical and Potentiometric Methods

Shoma Kuga, Jung-Hoon Yang, Hironori Takahashi, Kazuyuki Hirama, Takayuki Iwasaki, and Hiroshi Kawarada*

Department of Nano-Science and Nano-Engineering, School of Science and Engineering, Waseda University, 3-4-1 Okubo, Shinjuku-ku, Tokyo 169-8555, Japan, and Nanotechnology Research Center & Institute of Biomedical Engineering, Waseda University, Waseda Tsurumaki-cho 513, Shinjuku-ku, Tokyo 162-0041, Japan

Received November 9, 2007; E-mail: kawarada@waseda.jp

Abstract: The effects of surface charge density on DNA hybridization have been investigated on a mixture of hydrogen-, oxygen-, and amine-terminated diamond surfaces. A difference in the hybridization efficiencies of complementary and mismatched DNA was clearly observed by fluorescence and potentiometric observations at a particular coverage of oxygen. In the fluorescence observation, singly mismatched DNA was detected with high contrast after appropriate hybridization on the surface with 10−20% oxygen coverage. The amount of oxygen in the form of $C-O^-$ (deprotonated C−OH) producing the surface negative-charge density was estimated by X-ray photoelectron spectroscopy. Electrolyte solution gate field-effect transistors (SGFETs) were used for potentiometric observations. The signal difference (change in gate potential) on the SGFET, which was as large as ∼20 mV, was caused by the difference in the hybridization efficiencies of complementary target DNA (cDNA) and singly mismatched (1MM) target DNA with a common probe DNA immobilized on the same SGFET. The reversible change in gate potential caused by the hybridization and denaturation cycles and discriminating between the complementary and 1MM DNA targets was very stable throughout the cyclical detections. Moreover, the ratio of signals caused by hybridization of the cDNA and 1MM DNA targets with the probe DNA immobilized on the SGFET was determined to be 3:1 when hybridization had occurred (after 15 min on SGFET), as determined by real-time measurements. From the viewpoint of hybridization kinetics, the rate constant for hybridization of singly mismatched DNA was a factor of ∼3 smaller than that of cDNA on this functionalized (oxidized and aminated) diamond surface.

Introduction

As diamond has many attractive characteristics, such as a wide potential window,[1,2] physicochemical stability,[3,4] biocompatibility,[3−5] and potential for simple surface modification,[6−9] it has been expected to be useful for application in sensor devices, particularly those for biological materials. For example, DNA hybridization can be detected by fluorescence observation after a number of hybridization and denaturation cycles on the diamond surface, and the degree of degradation of the fluorescence signals is less than that observed on a silicon or gold substrate.[3,5] This is advantageous for the development of DNA chips with a diamond substrate for use in monitoring of fluorescent signals. The development of a label-free DNA sensor using diamond is also expected because a hydrogen-terminated (H-terminated) diamond surface with an undoped p-type conductive layer can be used for electrochemical analysis. In this work, mismatched DNA was detected successfully on both micropatterned diamond and diamond electrolyte solution gate field-effect transistors (SGFETs). A SGFET[10] is a p-channel FET using a p-type surface accumulation layer and is similar to FET-type sensors such as silicon-based ion-sensitive FETs (ISFETs). Although the gate insulator of silicon-based ISFETs should be covered by passivation films (SiN_4 or Al_2O_3) in order to prevent the intrusion of ions from the electrolyte solution to the gate insulator,[11,12] diamond SGFETs do not require insula-

(1) Pleskov, Y. V.; Sakharova, A. Y.; Krotova, M. D. *J. Electroanal. Chem.* **1987**, *228*, 19–27.
(2) Shin, D.; Watanabe, H.; Nebel, C. E. *Diamond Relat. Mater.* **2006**, *15*, 121–128.
(3) Yang, W.; Auciello, O.; Butler, J. E.; Cai, W.; Carlisle, J. A.; Gerbi, J. E.; Gruen, D. M.; Knickerbocker, T.; Lasseter, T. L.; Russell, J. N.; Smith, L. M.; Hamers, R. J. *Nat. Mater.* **2002**, *1*, 253–257.
(4) Härtl, A.; Schmich, E.; Garrido, J. A.; Hernando, J.; Catharino, S. C.; Walter, S.; Feulner, P.; Kromka, A.; Steinmüller, D.; Stutzmann, M. *Nat. Mater.* **2004**, *3*, 736–742.
(5) Nebel, C. E.; Shin, D.; Rezek, B.; Tokuda, N.; Uetsuka, H.; Watanabe, H. *J. R. Soc. Interface* **2007**, *4*, 439–461.
(6) Zhang, G.-J.; Song, K.-S.; Nakamura, Y.; Ueno, T.; Funatsu, T.; Ohdomari, I.; Kawarada, H. *Langmuir* **2006**, *22*, 3728–3734.
(7) Yang, J.-H.; Song, K.-S.; Zhang, G.-J.; Degawa, M.; Sasaki, Y.; Ohdomari, I.; Kawarada, H. *Langmuir* **2006**, *22*, 11245–11250.
(8) Wang, H.; Griffiths, J.-P.; Egdell, R. G.; Monoleny, G. M.; Foord, S. J. *Langmuir* **2008**, *24*, 862–868.
(9) Wang, X.; Colavita, P. E.; Metz, K. M.; Butler, J. E.; Hamers, R. J. *Langmuir* **2007**, *23*, 11623–11630.
(10) Kawarada, H.; Araki, Y.; Sakai, T.; Ogawa, T.; Umezawa, H. *Phys. Status Solidi A* **2001**, *185*, 79–83.
(11) Han, Y.; Offenhauser, A.; Ingebrandt, S. *Surf. Interface Anal.* **2006**, *38*, 176–181.
(12) Prushothaman, S.; Toumazou, C.; Ou, C. P. *Sens. Actuators, B* **2006**, *114*, 964–968.

tion or passivation films on the channel surface.[13−17] The current from the source electrode to the gate electrode is blocked over a wide potential window (~3 V). Therefore, diamond SGFETs can be fabricated more easily than ISFETs and can be used to detect surface-charge changes, such as DNA hybridization, with ultrahigh sensitivity.

About 400 diseases can now be diagnosed by molecular analysis of nucleic acids, and this number is increasing every year. DNA chips for the rapid and highly sensitive detection of specific DNA sequences are strongly required for the development of new diagnostic techniques and new drugs based on individual genes. The potentiometric detection method is particularly favorable for rapid analysis that requires no labels or reagents.[18−20]

However, there are number of problems regarding the detection of mismatched DNA by such potentiometric methods. First, charges associated with ionized DNA in the electrolyte solution are screened by the counterions in solution at a rate of ~70% under some conditions.[18] This indicates that the creation of a suitable environment for DNA detection is necessary, and immobilization of DNA near solid surfaces is required for the potentiometric method, considering the effect of Debye length defined by the ion concentration in the electrolyte solution.[21] The second problem is that nonspecific DNA is adsorbed onto the solid/liquid interface in the detection area. Nonspecific binding of DNA is caused by an attractive Coulomb force and/or hydrophobic interaction between the DNA and the surface.[22,23] Hybridization-based DNA sensors require the elimination of nonspecific signals caused by such adsorption of DNA because the nonspecific DNA also generates a signal of target DNA that suppresses the sensitivity of the sensors with respect to detection of the changes caused by specific hybridization of target DNA. The number of physisorbed molecules is related to the surface characteristics, such as surface charge state and hydrophobic−hydrophilic balance. For example, negatively charged molecules are adsorbed preferentially onto positively as opposed to negatively charged surfaces. Amphipathic molecules are adsorbed onto hydrophilic surfaces via contact between their hydrophilic groups and the surface.[24,25]Therefore, surface functionalization is frequently carried out to control the physisorption of biomolecules.[26−29] Third, the density of DNA immobilized on the surface is related to the sensitivity of the sensors to mismatched DNA. Although various technologies for immobilizing DNA on a substrate, such as fabrication of amino groups on a substrate and the use of linker molecules[19,30,31] or gold (substrate)−thiol group (functionalized to DNA) interactions,[32,33] have been used, it is still difficult to control the density of DNA immobilized on the surface. An example of detecting mismatched DNA is the use of a large polymer called a dendrimer as a linker molecule. This can allow the distance between immobilized DNAs to be controlled. The results of one study indicated that singly mismatched DNA can be identified if the interval between the amino groups is ~6 nm.[34] Thus, it is thought that mismatched DNA can be detected by controlling the density of the immobilized probe DNA. In addition, various methods such as atomic force imaging,[30] fluorescence imaging,[6,31,34] and the electrochemical method[19,26] have been reported. However, it is difficult to detect mismatched DNA with high accuracy with techniques other than surface plasmon resonance (SPR).

The stringency of nucleic acid interactions is affected by the electric field, which induces nucleic acid molecule transport and defines the concentration of negative charges of nucleic acids near the solid surface and the hybridization efficiency.[35] The attractive force of the electric field increases the rate of duplex formation compared with that in the absence of such a field, even for mismatched DNAs. This indicates that hybridization in an attractive field should make it difficult to discriminate between complementary DNA (cDNA) and mismatched DNA. On the other hand, the repulsive force induces rapid removal of incompletely hybridized molecules and enhances the denaturation of incomplete pairs more than that of complete pairs.[36] The repulsive potential (−300 mV) preferentially denatures mismatched DNA hybrids while leaving the fully complementary hybrids largely intact. Therefore, the electric field provided by a potential difference near the solid surface is one of the key issues in the control of DNA hybridization or denaturation and thus for detection of mismatched DNA with high sensitivity.

In this study, probe DNAs were immobilized directly on the solid surfaces to make use of the effect of the surface potential. By controlling the buffer solution, the immobilized probe DNAs can be located within the depth of the Debye length, and thus, target DNA movement during hybridization is strongly affected by the surface potential. For example, the electrostatic force of

(13) Song, K. S.; Sakai, T.; Kanazawa, H.; Araki, H.; Umezawa, H.; Tachiki, M.; Kawarada, H. *Biosens. Bioelectron.* **2003**, *19*, 137–140.
(14) Song, K. S.; Degawa, M.; Nakamura, Y.; Kanazawa, H.; Umezawa, H.; Kawarada, H. *Jpn. J. Appl. Phys.* **2004**, *43*, L814–L817.
(15) Song, K. S.; Nakamura, Y.; Sasaki, Y.; Degawa, M.; Yang, J. H.; Kawarada, H. *Anal. Chim. Acta* **2006**, *573−574*, 3–8.
(16) Sakai, T.; Song, K. S.; Kanazawa, H.; Nakazawa, H.; Umezawa, H.; Tachiki, M.; Kawarada, H. *Diamond Relat. Mater.* **2003**, *12*, 1971–1975.
(17) Kanazawa, H.; Song, K. S.; Sakai, T.; Nakazawa, Y.; Tachiki, M.; Kawarada, H. *Diamond Relat. Mater.* **2003**, *12*, 618–622.
(18) Poghossian, A.; Cherstvy, A.; Ingebrant, S.; Offenhausser, A.; Schoning, M. J. *Sens. Actuators, B* **2005**, *111*, 470–480.
(19) Drummand, T. G.; Michael, G. H.; Jaqueline, K. B. *Nat. Biotechnol.* **2003**, *21*, 1192–1199.
(20) Uno, T.; Tabata, H.; Kawai, T. *Anal. Chem.* **2007**, *79*, 52–59.
(21) Song, K. S.; Zhang, G. J.; Nakamura, Y.; Furukawa, K.; Hiraki, T.; Yang, J. H.; Funatsu, T.; Ohdomari, I.; Kawarada, H. *Phys. Rev. E* **2006**, *74*, 041919.
(22) Allahverdyan, A. E.; Gevorkian, Z. S.; Hu, C.; Nieuwenhuizen, T. M. *Phys. Rev. Lett.* **2006**, *96*, 098302.
(23) Carre, A.; Lacarriere, V.; Birch, W. *J. Colloid Interface Sci.* **2003**, *260*, 49–55.
(24) Ulman, A. *Chem. Rev.* **1996**, *96*, 1533–1554.
(25) Lussi, J. W.; Michel, R.; Reviakine, I.; Falconnet, D.; Goessl, A.; Csus, G.; Hubbell, J. A.; Textor, M. *Prog. Surf. Sci.* **2004**, *76*, 55–69.
(26) Zang, J.; Song, S.; Zang, L.; Wang, L.; Wu, H.; Pan, D.; Fan, C. *J. Am. Chem. Soc.* **2006**, *128*, 8575–8580.
(27) Tachiki, M.; Kaibara, Y.; Shigeno, M.; Kanazawa, H.; Banno, T.; Song, K. S.; Umezawa, H.; Kawarada, H. *Phys. Status Solidi A* **2003**, *199*, 39–43.
(28) Andruzzi, L.; Nickel, B.; Schwake, G.; Radler, J. O.; Sohn, K. E.; Mates, T. E.; Kramer, J. E. *Surf. Sci.* **2007**, *601*, 4984–4992.
(29) Park, S.; Lee, K. B.; Choi, I. S.; Langer, R.; Jon, S. *Langmuir* **2007**, *23*, 10902–10905.
(30) Rezek, B.; Shin, D.; Nakamura, T.; Nebel, C. E. *J. Am. Chem. Soc.* **2006**, *128*, 3884–3885.
(31) Knickerbocker, T.; Strother, T.; Schwartz, M. P.; Russell, J. N., Jr.; Butler, J.; Smith, L. M.; Hamers, R. J. *Langmuir* **2003**, *19*, 1938–1942.
(32) Rho, A.; Jahng, D.; Lim, J. H.; Choi, J.; Chang, J. H.; Lee, S. C.; Kim, K. J. *Biosens. Bioelectron.* **2008**, *23*, 852–856.
(33) Love, J. C.; Estroff, L. A.; Kriebel, J. K.; Nuzzo, R. G.; Whitesides, G. M. *Chem. Rev.* **2005**, *105*, 1103–1169.
(34) Hong, B. J.; Sunkara, V.; Park, J. W. *Nucleic Acids Res.* **2005**, *33*, e106.
(35) Gurtner, C.; Tu, E.; Jamshidi, N.; Haigis, R. W.; Onofrey, T. J.; Edman, C. F.; Sosnowski, R.; Wallace, B.; Heller, M. J. *Electrophoresis* **2002**, *23*, 1543–1550.
(36) Heaton, R. J.; Peterson, A. W.; Georgiadis, R. M. *Proc. Natl. Acad. Sci. U.S.A.* **2001**, *98*, 3701–3704.

Table 1. DNA Nomenclature and Sequences

name	sequence
For Optical Detection	
Comp. probe DNA	HOOC-5′-CCACGGACTACTTCAAAACTA-3′
1MM probe DNA	HOOC-5′-CCACGGACTAGTTCAAAACTA-3′
3MM probe DNA	HOOC-5′-CCAGGGACTAGTTCAATACTA-3′
Noncomp. probe DNA	HOOC-5′-ATCGATCGATCGATCGATCGA-3′
Comp. target DNA	3′-GGTGCCTGATGAAGTTTTGAT-5′-Cy5
For Potentiometric Detection	
Comp. probe DNA	HOOC-5′-CCACGGACTACTTCAAAACTA-3′
Comp. target DNA	3′-GGTGCCTGATGAAGTTTTGAT-5′
1MM target DNA	3′-GGTGCCTGATCAAGTTTTGAT-5′
Noncomp. target DNA	3′-ATGCATGCATGCATGCATGCA-5′

the surface negative charge repels DNA molecules approaching the surface, suppresses DNA physisorption, and retards hybridization. This repulsive force is the same as that produced by the electric field described above, but it is only effective when the probe DNA is immobilized close to the surface. We chose direct DNA immobilization without linker molecules and used oxygen atoms, which have a higher electronegativity than carbon atoms, as surface terminators. Even a partially oxidized diamond surface can reduce the surface potential by negatively charged oxygen termination on the H-terminated surface, which is relatively positively charged. The hybridization of target DNA with probe DNA becomes limited in perfectly matched pairs when the electrostatic attractive force is weakened by a partially oxidized diamond surface. This surface provides more stability than the H-terminated surface.

Experimental Methods

Chemicals and Oligonucleotides. DNAs were purchased from Sigma Genosis Company (Hokkaido, Japan). The 5′ ends of all of the probe DNAs were terminated with a carboxyl group. Without the use of linker molecules, this carboxyl group can bond the DNA and amine-terminated diamond directly and covalently. The end of the target DNA used for optical measurement by fluorescence microscopy was labeled with Cy5. The DNAs used for two experiments, fluorescence observation and SGFET measurement, were 21-mers. Table 1 shows the sequences of the DNAs. In the fluorescence observations, four types of probe DNA were immobilized on the diamond substrate: complementary (Comp.), singly mismatched (1MM), triply mismatched (3MM), and noncomplementary (Noncomp.) with respect to the target DNA (see Table 1). A fluorescent signal of distinct intensity could be observed on one substrate. In the SGFET measurements, common probe DNAs were immobilized on the channel surface, and three types of target DNA [Comp., 1MM, and Noncomp. (see Table 1)] were hybridized to the probe DNA, after which the SGFET signal (the change in the gate potential) was observed. Table 1 also shows the sequences of target DNAs used in the SGFET measurements.

Synthesis of H-Terminated Diamond Surface and Partial Functionalization with Ultraviolet Irradiation. Polycrystalline diamonds purchased from Element Six Co. Ltd. were used in this study. These are free-standing, transparent diamonds (so-called "optical grade") with a thickness of 300 μm and a large grain size ($\sim$100 μm) grown by the chemical vapor deposition method. The details of the growth parameters were not disclosed. Their surfaces were sufficiently flat for fabrication of high-performance FETs with a high cutoff frequency.[37,38] These substrates were H-terminated using a hydrogen plasma. The sheet resistance and carrier concentration of these substrates were 10−20 kΩ/square and $1-3 \times 10^{13}$ cm^{-2}, respectively, at room temperature, as determined by direct-current Hall Effect measurement.

Partial surface oxidation and amination of the H-terminated diamond was performed by irradiation with UV light. Nitrogen gas was introduced into the reaction chamber for 5 min to remove activated gases. Introduction of oxygen gas into the chamber was followed by UV irradiation for 30 min. The UV source was a mercury lamp, and the wavelength used was 184.9 nm. Amino groups were formed on the partially oxidized diamond substrate in an ammonia gas chamber. After nitrogen was introduced into the chamber, ammonia gas (99.9%) was introduced at 100 sccm and the substrate irradiated with UV light for 1 h. The UV source was low-pressure mercury, and the wavelength used was 253.7 nm. These procedures were performed at room temperature, and it was unnecessary to evacuate the chamber, allowing the modification to be performed in a short time. This is the advantage of surface modification using UV irradiation. It does not cause damage to the diamond substrate, because the modification occurs very slowly.

Evaluation of the Degree of Surface Modification by X-ray Photoelectron Spectroscopy. The extents of oxygen and nitrogen coverage on the diamond surface were evaluated by X-ray photoelectron spectroscopy (XPS). The X-ray photoelectron spectroscope used in this study was an Ulvac Φ 3300 (Ulvac-Phi, Kanagawa, Japan) equipped with an Al Kα X-ray source. The electron takeoff angle was 45 $\pm$ 3° relative to the substrate surface after focusing of the monochromator irradiation on the sample, and the slit width was kept constant at 1.1 mm. The coverage of nitrogen was calculated from the ratio of the C1s and N1s peak areas. The coverage of oxygen (O1s, 532.6 eV) was determined by deconvolution of the C1s peak intensity. The X-ray was monochromatized, and its half-bandwidth was 0.1 eV.

Detection of Mismatched DNA by Fluorescence Microscopy. For detection of mismatched DNA by fluorescence observations, a micropattern on a modified surface was fabricated by photolithography. Figure 1 shows the 20 μm diameter Au dots. Au was deposited by evaporation onto the diamond surface at a thickness of $\sim$100 nm, and a photoresist (OFPR-800) was used to coat the surface for use in the photolithography technique. After the pattern was formed by UV photolithography, Au was etched off with KI solution. The set of circular Au dots acted as a metal mask to protect the surface from fluorination using inductively coupled plasma (ICP) (RIE-101PH, Samco International Inc., Kyoto, Japan). After the ICP treatment with C_3F_8 gas, the surface outside the Au dots was fluorine-terminated to minimize the physical adsorption of DNAs on the background surface. As the fluorine-terminated surface is negatively charged [because of the difference in the electronegativities of fluorine (4.0) and carbon (2.5)] and also superhydrophobic, nonspecific adsorption of probe and target DNA was minimal.[6] The C_3F_8 plasma treatment was carried out for 50 s with C_3F_8 gas at a flow rate of 20 sccm, a chamber pressure of 3 Pa, an ICP power of 500 W, and a bias of 20 W. After the gold mask was etched with KI solution, the surface was rinsed in water three times to remove the iodide ions adsorbed on the surface. The adsorbed iodide ions may not have been perfectly decontaminated, but no effects of remaining iodide ions were observed in our previous studies[6,7] or in the results described in this paper. This process was not used to fabricate the diamond SGFET,[10] and therefore, iodide ions did not affect the FET properties. The four types of probe DNA (Table 1) were immobilized onto the micropatterned substrate. The final concentration of the immobilized probe DNA was 10 μM because the concentration of probe DNA was 20 μM in 2× sodium saline citrate (SSC) buffer solution, and 0.1 M *N*-hydroxysuccinimide (NHS) and 0.4 M 1-ethyl-3-(3-dimethylaminopropyl)carbodiimide hydrochloride (EDC) were added to this solution at 25% (v/v). Next, probe DNAs were immobilized on the surface via amide bond formation between the DNA carboxyl groups and the amino groups on the diamond surface. DNA immobilization was carried out for 2 h at 38 °C in a humidified chamber. After immobilization,

(37) Ueda, K.; Kasu, M.; Yamauchi, Y.; Makimoto, T.; Schwitters, M.; Twitchen, D. J.; Scarsbrook, G. A.; Coe, S. E. *Diamond Relat. Mater.* **2006**, *15*, 1954–1957.
(38) Hirama, K.; Takayanagi, H.; Yamauchi, S.; Yang, J. H.; Kawarada, H.; Umezawa, H. *Appl. Phys. Lett.* **2008**, *92*, 112107.

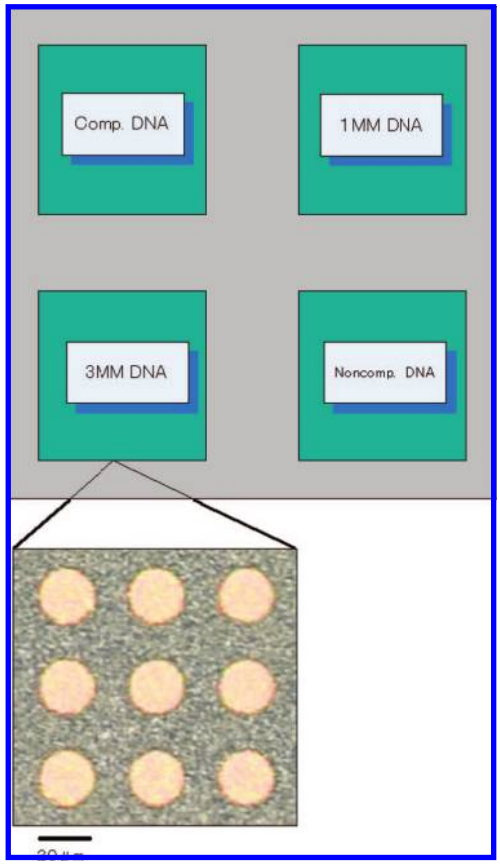

Figure 1. Schematic of a substrate fabricated for optical experiments using fluorescence microscopy. Micropatterns were fabricated in four parts on a 1.4 × 1.4 cm polycrystalline diamond substrate. The inside of each dot was partially functionalized with oxygen and ammonia, and outside of each dot was the fluorine-terminated surface. Each dot was 20 μm in diameter, and the dot interval was 10 μm.

the substrate was washed once in phosphate-buffed solution (PBS) with Tween-20 and three times in water at room temperature to remove physisorbed probe DNA on the surface, and then target DNA labeled with Cy5 was hybridized to the directly immobilized probe DNA. The concentration of target DNA was 100 nM in 2× SSC buffer solution, and the hybridization temperature was 55 °C. The hybridization times were 10, 20, and 30 min. After target DNA hybridization, the substrate was washed in 2× SSC buffer with 10% sodium dodecyl sulfate, then in 2× SSC buffer, and finally in 0.2× SSC buffer for 5 min to remove nonspecifically adsorbed DNA. Fluorescence observations were performed using an epif-luorescence microscope (Olympus IX71, Olympus, Tokyo, Japan).

Detection of Mismatched DNA Using SGFETs. SGFETs were fabricated as follows. A 150 nm thick film of Au was deposited by evaporation onto the H-terminated surface through a metal mask to serve as source and drain electrodes. Then, Ar^+ ions were implanted through the metal mask to form an insulating region outside the metal electrodes. The acceleration voltage for the implantation was 25 keV, and the density of dosed ions was 2×10^{14} cm^{-2}. The dosed region was highly resistive at this ion density[39] and did not form graphitic defects, which can be found at ion densities greater than 10^{16} cm^{-2} and exhibit strong electrochemical properties. Therefore, the electrochemical activity region was not formed in the implanted region. Wires were bonded to the drain and source electrodes using electroconductive paste and covered with epoxy resin to protect them from the electrolyte solution. The channel surface was exposed to the electrolyte solution. The length and width of the gate channel were 500 μm and 8 mm, respectively.

(39) Hokazono, A.; Kawarada, H. *Jpn. J. Appl. Phys.* **1997**, *36*, 7133–7139.

Table 2. Hybridization, Denaturation, and Measurement Conditions

measurement	process	buffer solution	NaCl concentration (M)	temperature (°C)
fluorescence	hybridization	2× SSC	0.3	55
	measurement	−	−	RT
static	hybridization	2× SSC	0.3	55
	measurement	PBS	0.001	RT
real-time	hybridization/ measurement	1× SSC	0.15	RT
all	denaturation	10 min in 8.3 M urea solution		RT

Hybridization of target DNA to probe DNA was detected using data on the static characteristics and the time-dependent gate potential changes (real-time measurement) of the SGFETs. The probe DNA shown in Table 1 was immobilized onto the surface of the gate channel of the diamond SGFET using a method similar to that for optical detection via fluorescence microscope. The static characteristics of the SGFET were determined in 1 mM PBS using an Ag/AgCl reference electrode as the gate electrode. Drain current (I_{ds}) as a function of gate voltage (V_{gs}) was determined at a constant drain-source voltage (V_{ds}) of −0.1 V. The detection of mismatched DNA on a SGFET was performed in two ways: static measurement and real-time measurement. In the static measurement, Comp. and 1MM DNA were hybridized to immobilized probe DNA in a humidity-controlled chamber (55 °C). After the channel surface was washed by the same method as in the determination of denaturation characteristics, the change in V_{gs} at constant I_{ds} was evaluated. For denaturation of target DNA, the SGFET channel was exposed to 8.3 M urea for 10 min and then rinsed three times in water for 5 min.[21] In the real-time measurement, 72 μL of 1× SSC buffer solution was placed in the SGFET channel where the probe DNA was immobilized, and the shift in V_{gs} was measured at $I_{ds} = -8$ μA with $V_{ds} = -0.1$ V; target DNA was injected 2 min later, when V_{gs} had stabilized. The injected target DNA concentration was 1 μM in 1× SSC buffer solution, and the amount of injected solution was 8 μL. The final target DNA concentration reached 100 nM during hybridization. Upon hybridization of target DNA to immobilized probe DNA, more holes emerged in the surface conductive layer because of the increased negative charge of the surface, and the conductivity between the drain and source electrodes increased. Therefore, V_{gs} shifted in the positive direction, and this gate-potential shift was evaluated. Denaturation was carried out in 8.3 M urea for 10 min (i.e., the same conditions used for the static measurement). The three types of target DNA (Table 1) were injected into the same SGFET to evaluate differences in hybridization affinity and kinetics between complementary and mismatched DNAs. Only 1 × SSC buffer solution was injected to determine the reference gate voltage shift of the drift characteristic of SGFET, and the changes in V_{gs} over time were determined. The conditions, solution concentrations, and temperatures used in the experiment are summarized in Table 2.

Results and Discussion

Evaluation of the Degree of Surface Modification by XPS. To evaluate the modified surface and surface charge, we determined the coverages of oxygen and nitrogen on the diamond surface by XPS. Figure 2 shows the XPS results for an aminated, partially oxygen-terminated surface. Figure 2a shows a wide scan of the surface, in which the main C1s peak (285 eV) and the O1s (537.5 eV) and N1s peaks (399.9 eV) can be seen. The amino group and oxygen coverages were estimated from the ratio of peak areas, such as N1s (Figure 2b) to C1s or O1s (Figure 2c) to C1s. The amino group and oxygen coverages on this surface were confirmed by this calculation to be 13 and 50%, respectively. However, the O1s peak area

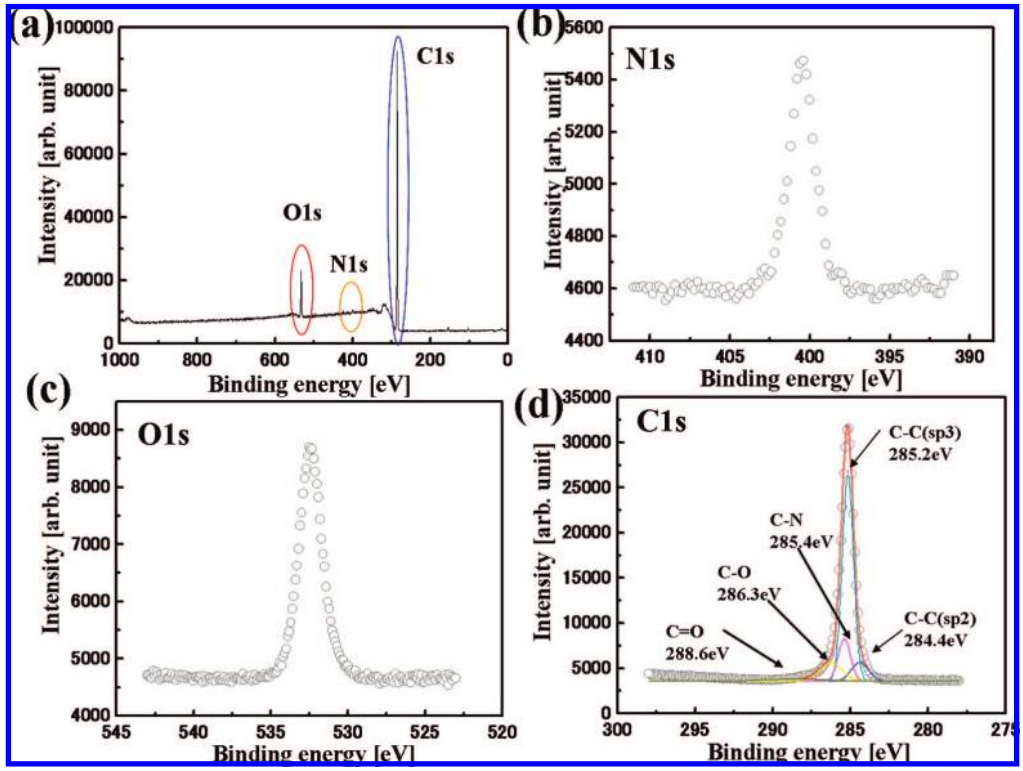

Figure 2. (a) XPS survey scan over the binding energy ranges 0−1000 eV. The O1s, N1s, and C1s peaks from the oxygen terminations, amino groups, and diamond substrate, respectively, were detected. (b) High-resolution scan of the N1s peak. (c) High-resolution scan of the O1s peak. (d) High-resolution scan of the C1s peak, on which deconvolution was performed in order to evaluate the coverages of oxygen termination. The ratios of the areas of the peaks for the various bonding types reflect the coverages of the functionalized groups.

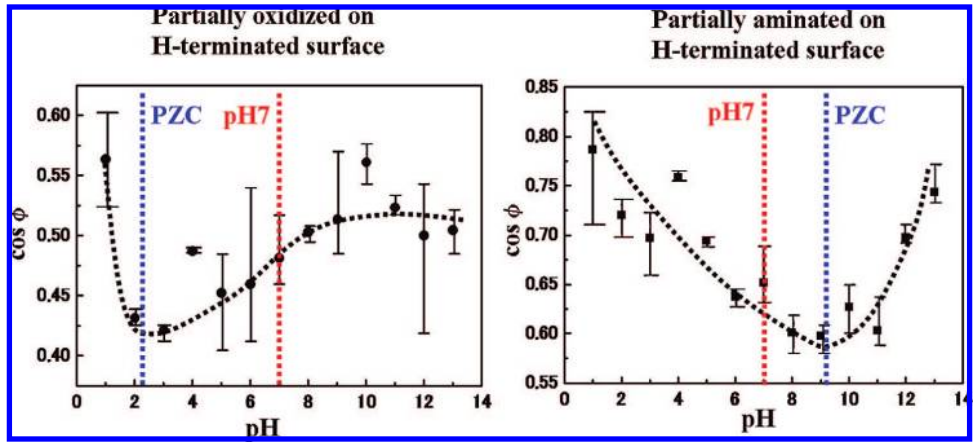

Figure 3. Plots of the cosine of the contact angle value as a function of pH on (a) partially oxidized and (b) partially amine-terminated diamond surfaces. The PZCs of the two surfaces were pH 2 and 9, respectively. A surface is positively charged at a pH below the PZC and negatively charged at a pH above the PZC. Therefore, the partially oxidized H-terminated surface was negatively charged and the partially aminated H-terminated surface was positively charged in our experiments at pH 7.

included contributions from oxygen terminations, such as C−O and C═O bonding, and oxygen atoms in water molecules. The adsorbed water on the diamond surface is not negligible on hydrophilic surfaces such as these oxygen- and amine-terminated ones. To evaluate the oxygen-termination contribution to the O1s peak, deconvolution of the C1s peak was performed, as shown in Figure 2d. The main peak at 285.2 eV corresponds to the C−C (sp^3) bonds of diamond.[40,41] The C−H bonds could not be detected by XPS measurement, because XPS cannot detect H atoms. The positions of the peaks at 285.4, 286.3, and 288.6 eV correspond to C−N, C−O, and C═O bonds, respectively,[42,43] on the functionalized diamond surface. However, the deconvolution of C−C (sp^3) and C−N is difficult because the difference in the binding energies for these bonds is quite small (0.2 eV). Therefore, the C−O and C═O peaks were fitted after the C−N peak was assumed to contribute 13%, as calculated from the N1s-to-C1s peak-area ratio. From these results, the coverages of C−O and C═O were 13 and 3%,

(40) Diaz, J.; Paolicelli, G.; Ferrer, S.; Comin, F. *Phys. Rev. B* **1996**, *45*, 8064–8069.
(41) Paik, N. *Surf. Coat. Technol.* **2005**, *200*, 2170–2174.
(42) Abdul majeed, R. M. A.; Datar, A.; Bhoraskar, S. V.; Bhoraskar, V. N. *Nucl. Instrum. Methods Phys. Res., Sect. B* **2007**, *258*, 345–351.
(43) Sahoo, R. R.; Patnaic, A. *Appl. Surf. Sci.* **2005**, *245*, 26–38.

Table 3. Quantification of Bonding States on the Surface

bonding state	binding energy (eV)	coverage (%)
C−C (sp^2)	284.2	3
C−C (sp^3)	285.2	68
C−N	285.4	13
C−O	286.3	13
C═O	288.6	3

respectively. The coverages calculated from these calculations are summarized in Table 3. The coverages of hydrogen termination, amino groups, and oxygen termination on the diamond surface were 68, 13, and 16%, respectively; these values represent the means for three identical samples. The surface hole accumulation originated from the 68% coverage of hydrogen and was sufficient to operate the FET. The oxygen coverage estimated from the ratio of O1s to C1s in this study (∼50%) exceeds that previously reported[7,15] on directly aminated H-terminated surfaces (∼10%). Therefore, the effect of the oxidation process in this experiment was very large.

Determination of Surface Charge State from Contact-Angle Measurements. The surface isoelectric point is useful in estimating the surface charge state. On the hydroxyl group surface (C−OH), the ionized bonds are present as $C-O^-$ or $C-OH_2^+$ in buffer solution. At pH 7, the density of the former is found to be 10^{10} times higher than the latter, as discussed later. The hydroxyl group surface acquires an ionic charge by the following reactions:

$$C-OH_2^+ + H_2O \rightleftarrows C-OH + H_3O^+ \quad (1)$$

$$C-OH + H_2O \rightleftarrows C-O^- + H_3O^+ \quad (2)$$

Adding eqs 1 and 2 yields

$$C-OH_2^+ + 2H_2O \rightleftarrows C-O^- + 2H_3O^+ \quad (3)$$

for which the equilibrium constant K_T is given by

$$K_T = \frac{\Gamma_{C-O^-}[H_3O^+]^2}{\Gamma_{C-OH_2^+}} \quad (4)$$

where Γ_{C-O^-} and $\Gamma_{C-OH_2^+}$ are the surface densities of deprotonated and protonated hydroxyl groups, respectively. $[H_3O^+]$, which is the concentration of hydronium ions (protons) in solution, is related to the pH of the probe solution. K_T measures the strength of the proton attraction by the hydroxyl groups and can be calculated via the pH of the point of zero charge (PZC) on the surface. When the pH near the surface is higher than the PZC, the majority of the hydroxyl groups exist as $C-O^-$. In contrast, when the pH near the surface is lower than the PZC, the majority exist as $C-OH_2^+$. This change in the charge state of the hydroxyl group is the origin of the pH-dependent surface tension discussed later. The ratio of $C-O^-$ can be obtained from measurements of the contact angle by changing the pH of the probe solution.[44] Protons adsorbed to or desorbed from the hydroxyl groups change the surface ionicity. The ratio of the change in contact angle to the change in pH of the dropped solution reflects the ionized hydroxyl groups and the adsorption of hydroxide ions on the surface. The amount of adsorption or desorption of protons (i.e., $\Gamma_{C-OH_2^+}$ or Γ_{C-O^-}, respectively) and the amount of adsorption of hydroxide ions can be described with the Young and Gibbs equations and by the expression

$$\Gamma = \frac{\gamma}{2.303RT}\frac{d(\cos\phi)}{d(pH)} \quad (5)$$

where γ is the surface tension of probe solution, R and T are the gas constant and absolute temperature, respectively, ϕ is the contact angle, and Γ is the amount of surface charge caused by the desorbed or adsorbed proton and the adsorption of hydroxide.[44] Therefore, if $d(\cos\phi)/d(pH)$ has a positive or negative value, the surface charge is negative or positive, respectively. Equation 5 indicates that the number of adsorbed protons is proportional to the derivative of $\cos\phi$ with respect to the pH. Figure 3 shows a plot of $\cos\phi$ versus pH. The pH was controlled using NaOH and H_2SO_4 solution because the effects of Na^+ and SO_4^{2-} on the surface potential of the functionalized diamond are small if the background electrolyte is a dilute solution. On the H-terminated surface, the dependence of the surface potential on the Na^+ concentration was investigated previously[16,17,45] and found to be small[45] or not detected;[16,17] it was not detected on the partially oxidized surface either.[16] Changes in surface potential on a functionalized diamond surface as a result of changing the SO_4^{2-} concentration have not been reported and can be considered to be small compared with the effect of adsorption of protons. On the partially oxidized surface, the derivative of $\cos\phi$ with respect to pH is positive near pH 7, as shown in Figure 3a, indicating a negatively charged surface. The hydroxyl group proton is attractively desorbed into the solution, and the surface is almost completely ionized to $C-O^-$. As $\Gamma = 0$ at the PZC, it follows from eq 5 that

$$\frac{d(\cos\phi)}{d(pH)} = 0 \quad (6)$$

at the PZC. Therefore, a minimum in $\cos\phi$ will occur at the PZC as the pH of the probe solution is changed. The $\cos\phi$ value reaches a minimum at pH 2, in good agreement with the previous results of Härtl and co-workers,[45] who concluded that the isoelectric point of oxygen-terminated diamond is pH 1.5. Thus, K_T in eq 4 is equal to 10^{-4}, which further shows that protons are weakly held at the partially oxidized diamond surface. On the basis of the expression $\Gamma_{C-O^-}/\Gamma_{C-OH_2^+} = K_T/[H_3O^+]^2$ (obtained by rearranging eq 4), the K_T value of 10^{-4} indicates that the amount of $C-O^-$ on the surface (Γ_{C-O^-}) is $\sim 10^{10}$ times larger than the amount of $C-OH_2^+$ ($\Gamma_{C-OH_2^+}$) at pH 7, where most of the DNA hybridization was carried out in this study. The hydroxyl group functionalized on the surface was negatively charged under our experimental conditions, although the number of hydroxyl groups could not be determined by this contact angle measurement.[44] Ionization of amino groups ($C-NH_2$) on H-terminated surfaces was estimated using the same approach. The amino groups on the surface may acquire an ionic charge by the following reaction:[15]

$$C-NH_3^+ + H_2O \rightleftarrows C-NH_2 + H_3O^+ \quad (7)$$

The PZC of partially aminated H-terminated surfaces was confirmed to be pH 9 (Figure 3b). Therefore, the K_T value for eq 7 is 10^{-9}, which indicates that the number of protonated amino groups was 10^2 times larger than that of un-ionized amino groups at pH 7. Therefore, the partially aminated H-terminated surface had a globally positive charge in solution at pH 7.

(44) Chau, L. K.; Porter, M. D. *J. Colloid Interface Sci.* **1991**, *145*, 283–286.

(45) Härtl, A.; Garrido, J. A.; Nowy, S.; Zimmermann, R.; Werner, C.; Horinek, D.; Netz, R.; Stutzman, M. *J. Am. Chem. Soc.* **2007**, *129*, 1287–1292.

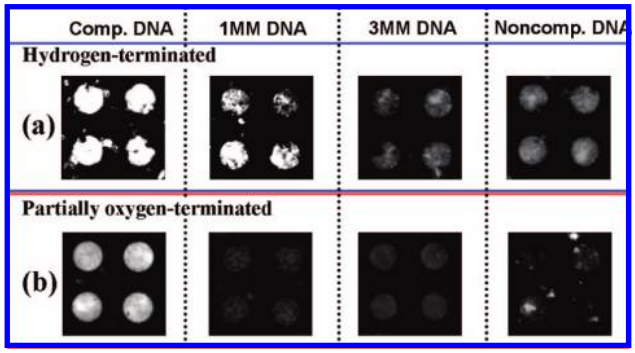

Figure 4. Detection of mismatched DNA by fluorescence intensity. (a) Aminated H-terminated surface. (b) Aminated partially O-terminated surface. The hybridization time was 30 min. The contrast between complementary (Comp.) and singly mismatched (1MM) DNAs was higher in (b) than in (a).

In view of the coverage of O^- and NH_3^+ at pH 7 on the partially aminated, partially oxidized diamond surfaces used as substrates for DNA hybridization in this study, positive and negative charges coexist on the surface. On average, the surface is approximately neutral because the coverages of amino-group and oxygen termination are on the same order. However, the negatively charged areas exist locally and affect the hybridization of DNA. Thus, the number of hydroxyl groups is the dominant determinant of the surface charge.

Detection of Mismatched DNA by Fluorescence Microscopy. The difference in DNA hybridization on H-terminated and partially O-terminated surfaces was examined by fluorescence microscopy (Figure 4). Two surfaces were used: one was directly aminated on the H-terminated surface (without the oxygenation process), and the other was aminated on the partially oxidized H-terminated surface. The hybridization times were 10, 20, or 30 min. Figure 4 shows the changes in termination of the two types of diamond surfaces after 30 min of hybridization. The density of the amino groups was the same (13%) on the two surfaces. However, the difference in the fluorescence intensities from hybridization of Comp. and 1MM DNAs with probe DNA was greater on the partially oxidized surface (Figure 4b) than on the directly aminated surface (Figure 4a). This result indicated that the partially oxidized diamond surface was suitable for detection of mismatched DNA.

This effect can be explained by considering the decrease in the attractive force between the diamond surface and the target DNA using a simple model based on the Gouy−Chapman−Stern theory, as shown schematically in Figure 5.[45] The potential difference between the diamond surface and the electrolyte solution was assumed to be identical for the partially aminated and partially oxygenated surfaces. The potential at the Helmholtz plane (ψ_H) shapes the potential profile in the solution close to the surface. Because of the protonated amino group, the partially aminated H-terminated surface is positively charged in solution at pH 7, as shown in Figure 5a, producing a large positive potential ψ_H at the Helmholtz plane. Outside this plane, the positive potential profile drops exponentially and shows a steep potential curve, as shown in Figure 5a. Therefore, negatively charged molecules, such as DNA, are subjected to an attractive force from the partially aminated surface because of the steep potential profile. This force can accelerate the hybridization of target DNA with probe DNA but is not beneficial for discrimination of mismatched DNA. On the other hand, the oxygen-terminated surface is negatively charged at pH 7, as shown in Figure 3a, and the surface potential is decreased compared with that of the surface with positive charge due to protonated amino groups. If the density of protonated amino groups is higher than that of deprotonated hydroxyl groups ($C-O^-$) providing a counter surface charge, the Helmholtz potential ψ_H approaches zero (i.e., the surface becomes neutralized), as shown by the red curve in Figure 5b. It has been reported that passive hybridization, i.e., hybridization without an external bias voltage, is more suitable for detecting mismatched DNA than that under an attractive field.[36] If the density of protonated amino groups is lower than that of deprotonated hydroxyl groups providing a negative surface charge, the Helmholtz potential ψ_H becomes negative, as shown by the blue curve in Figure 5b. This situation has already been discussed with regard to the low oxygen coverage (10%) of the H-terminated surface.[45] As the attractive field diminishes and the repulsive force emerges, the discrimination between mismatched DNA and cDNA is increased. Under the repulsive force, only perfectly matched DNA can hybridize with immobilized probe DNA. A similar phenomenon has been observed under an externally applied electric field that produces a repulsive force and thereby provides a suitable environment for discrimination of mismatched DNA from cDNA.[46,47] A harsh environment like the repulsive field is advantageous for the discrimination. Without control of the external voltage bias, O-terminated diamond has the same effect because of the negative charge from $C-O^-$ on the surface. The surface effect is made more pronounced by the short distance between the surface and the probe and corresponding target DNA, which results from the direct immobilization of the probe DNA.

This effect can be confirmed by comparing the two fluorescence images showing hybridization of Comp. DNA in Figure 4. The absolute intensity in Figure 4a is higher than that in Figure 4b, indicating that hybridization between probe and target DNAs is regulated by the presence of oxygen termination on the diamond surface. This indicates that the attractive field from the H-terminated surface increases the degree of target DNA hybridization. The difference in hybridization efficiency between Comp. and mismatched DNAs is due to the decrease in the thermodynamic stability of DNA double helices with base mismatches. Such phenomena have been demonstrated in experiments using SPR on gold thin films.[48]

Detection of Mismatched DNA Using SGFETs. Previously, we reported changes in the properties of semiconductive diamond surfaces resulting from functionalization of the surface.[16,49] The carrier density in the channel decreased gradually from 10^{13} to 10^8 cm^{-2} as a result of 20% oxygen coverage, but the channel mobility did not change drastically. It was confirmed that the transconductance (g_m) of SGFETs did not change significantly up to an oxygen coverage of 15%.[16,49] In the case of surface amination, the FET characteristics did not change for amine coverages up to 20%. The mobility decrease caused by Coulomb scattering was not distinct. The current flowing beneath the functionalized surface may be percolated by the fluctuating surface potential at $C-NH_3^+$ and/or $C-O^-$; although 10−20% coverage of these species shifted

(46) Sphehar-Deleze, A. M.; Schmidt, L.; Neier, R.; Kulmala, S.; Rooji, N. D.; Koudelica-Hep, M. *Biosens. Bioelectron.* **2006**, *22*, 722–729.
(47) Sosnowski, R. G.; Tu, E.; Butler, W. F.; O'Connell, J. P.; Heller, M. J. *Proc. Natl. Acad. Sci. U.S.A.* **1997**, *94*, 1119–1123.
(48) Peterson, A. W.; Heaton, R. J.; Georgiadis, R. *J. Am. Chem. Soc.* **2000**, *122*, 7837–7838.
(49) Kawarada, H. In *Thin Film Diamond II*; Nebel, C. E., Ristein, J., Eds.; Semiconductors and Semimetals, Vol. 77; Elsevier: Amsterdam, 2004; pp 328−332.

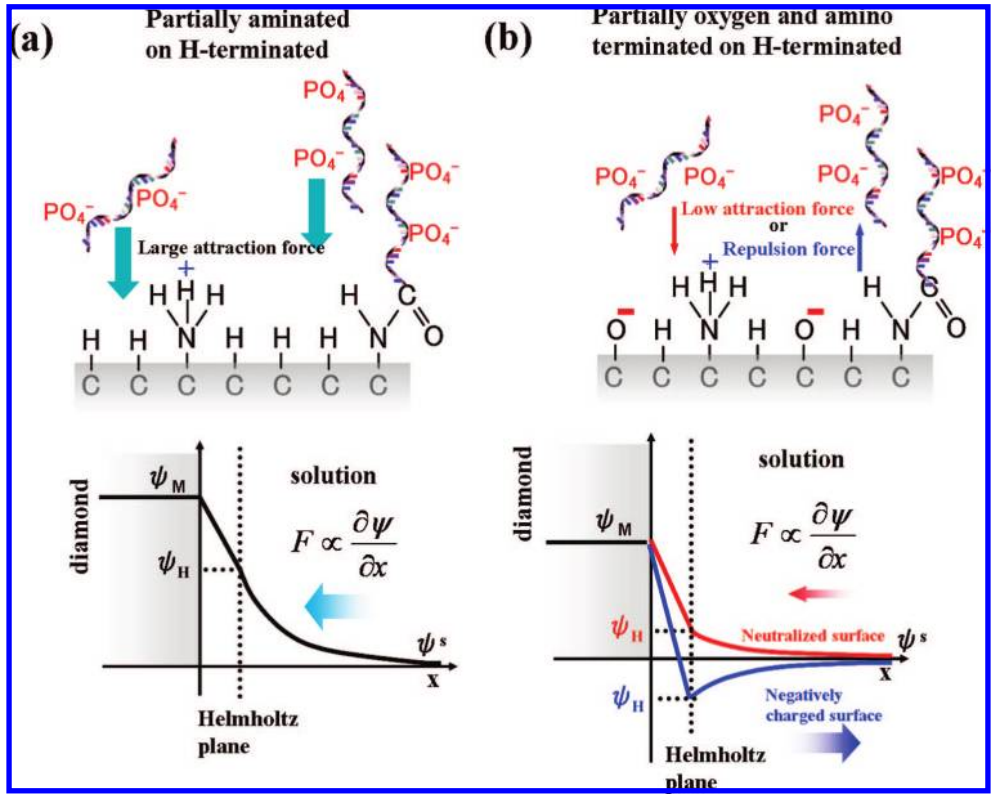

Figure 5. Schematic diagram illustrating the surface charge effect on target DNA movement. The potential difference between the diamond surface and the electrolyte solution is assumed to be identical on the partially aminated and partially oxygenated surfaces. The potential at the Helmholtz plane (ψ_H) shapes a potential profile in the solution close to the surface. (a) Surface with a positive charge due to protonated amino groups ($C-NH_3^+$) at pH 7. Negatively charged molecules such as DNA are attracted to the positively charged surface. Outside the Helmholtz plane, the positive potential profile drops rapidly and shows a steep potential curve. (b) Surface with a negative charge due to deprotonated hydroxyl groups ($C-O^-$) at pH 7. Mismatched target DNA is repelled, and only matched target DNA selectively hybridizes with probe DNA. The potential profile drops markedly at the Helmholtz plane. If the density of the protonated amino groups ($C-NH_3^+$) is lower than that of the dehydrogenated hydroxyl groups ($C-O^-$), the Helmholtz potential ψ_H becomes negative.

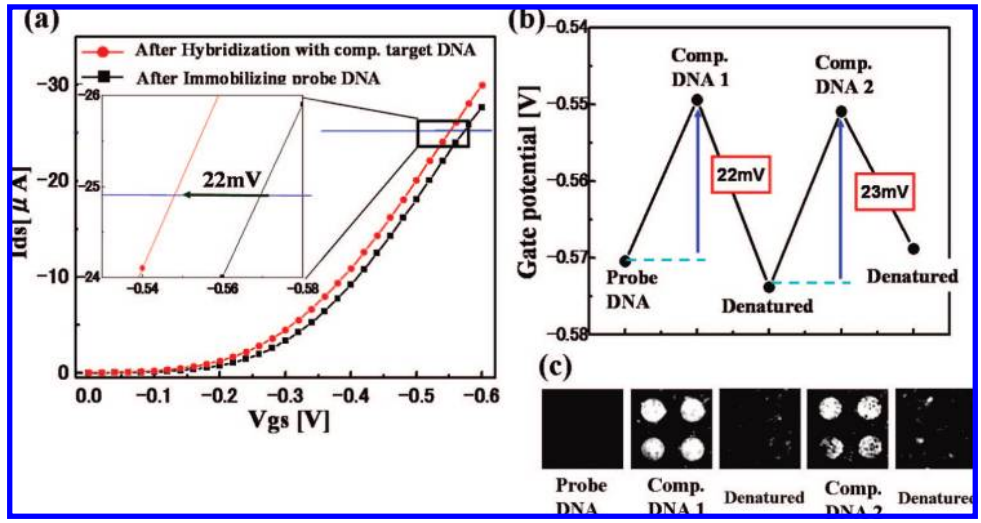

Figure 6. Static and transfer characteristics of a SGFET after hybridization and denaturation. (a) Static characteristics of the SGFET before and after DNA hybridization. The gate-potential shift upon hybridization of target DNA with immobilized probe DNA was observed at $I_{ds} = -25\ \mu A$ and found to be ~22 mV. (b) Transfer characteristics of the SGFET over two hybridization/denaturation cycles. The gate-potential shift was observed at $I_{ds} = -25\ \mu A$. In the first denaturation, the gate potential shifted negatively by ~23 mV, and the positive shift in gate potential upon rehybridization was ~23 mV. (c) Fluorescence observation of denaturation characteristics on a diamond surface. Double-stranded DNA was clearly denatured in urea solution.

the threshold voltage, the g_m did not change significantly. Kawarada[49] discussed these FET characteristics, particularly in Figure 16 in ref 49.

Other FET characteristics can be summarized as follows. The leakage current (I_{gs}) was less than 10 nA over the entire range of bias voltages (the detailed characteristics of I_{gs} are given in Figure S1 in the Supporting Information). The drift characteristic of the functionalized surface was determined by monitoring the time-dependent shift in the gate potential (V_{gs}). The drift in threshold voltage of partially oxidized or aminated SGFETs was

±3 mV after 8 h of operation, which was smaller than that of the SGFET with an H-terminated channel surface (see Figure S2 in the Supporting Information). In addition, the gate voltage in single-stranded DNA (as immobilized probe DNA or denatured DNA) preserved almost the same level. Therefore, the partially oxygen-terminated SGFET was sufficiently stable to detect many cycles of hybridization and denaturation in comparison with the H-terminated one. The shift in gate voltage was observed at $I_{ds} = -25\ \mu A$ and $V_{ds} = -0.1$ V. When target DNA hybridized to probe DNA, the shift in gate voltage was 22 mV, as shown in Figure 6a. As the conductance of the gate channel increased with hole density on the diamond surface (a result of an increase in the negative charge on the surface due to the intrinsic charge of hybridized target DNA), the gate voltage shifted in the positive direction.

Next, we quantified the density of immobilized probe DNA on the partially oxygen-terminated surface by two methods: using the Grahame equation and applying the theory of silicon-based ISFETs from the viewpoint of charge distribution in parallel capacitances that exist on the gate surface. In these calculations, we had to consider the influence of the counterion screening effect, which decreases the effect of changing the charge and the gate-voltage shift induced by hybridization of the target DNA. According to Manning's counterion condensation theory,[50] monovalent cations reduce the DNA charge by 76%. In addition, according to the Debye−Hückel theorem, the more diffuse ionic layer, where the charge density decreases exponentially with distance from the gate surface, compensates for the remaining charge.[18] These screening effects markedly decrease the charges associated with the hybridization of target DNA.

The Grahame equation describes the change in surface potential in terms of charge attachment to the surface.[51] We consider the total surface-potential change to be induced by the sum of the charges existing on each phosphate group in the DNA backbone with some distance from the surface. Applying the Grahame equation to the channel surface of the SGFET provides the following description of the signal transduced to the channel potential from the surface charge by attachment of charged molecules to the channel surface:[51,52]

$$\Delta V_{gs} = \sum_{j=1}^{n} \frac{2kT}{e}\left[\sinh^{-1}\left(\frac{\sigma_0 - \sigma_{NH_2-probeDNA} - \xi\sigma_{probeDNA}}{\sqrt{8\varepsilon_{elect}\varepsilon_0 kTn_0}}\right) - \sinh^{-1}\times \left(\frac{\sigma_0 - \sigma_{NH_2-probeDNA} - \xi\sigma_{probeDNA} - \xi_j(1-\theta)(\sigma_{targetDNA}/n)}{\sqrt{8\varepsilon_{elect}\varepsilon_0 kTn_0}}\right)\right] \quad (8)$$

where ΔV_{gs} is the shift in the channel potential after hybridization with target DNA, k is Boltzmann's constant, T is the absolute temperature, e is the elementary charge, ε_0 is the permittivity of vacuum, ε_{elect} is the dielectric constant of water (78), n_0 is the buffer ionic strength, σ_0 is the surface charge density, $\sigma_{probeDNA}$ is the immobilized DNA charge density on the surface, $\sigma_{NH_2-probeDNA}$ is the charge density of amino groups eliminated upon the immobilization of probe DNA, $\sigma_{targetDNA}$ is the charge density of hybridized target DNA, and ξ_j, ξ, and θ are factors related to the counterion screening effect. Equation 8 indicates that ΔV_{gs} is the sum of changes in gate voltage caused by the immobilized charges that exist on the gate surface at various distances r_j. As the Coulomb potential at a distance r_j from the charged molecule is decreased ξ_j times in electrolyte solution, ξ_j, the exponentially decreased factor of the charge effect with distance, is given by

$$\xi_j = \frac{e^{-r_j/\lambda_D}}{r_j} \quad (9)$$

where λ_D is the Debye length. Thus, the effect of charge density σ at a distance r_j from the surface is equal to the effect of a surface charge equal to $\xi_j\sigma$. Therefore, the effective charge (converted to surface charge density) of a 21-mer probe DNA is described by the expression

$$\xi\sigma_{probeDNA} = \sum_{j=1}^{21}\left(\frac{e^{-r_j/\lambda_D}}{r_j}\frac{1}{21}\sigma_{probeDNA}\right) \quad (10)$$

This expression states that the charges in the probe DNA are decreased by factors of ξ_j and that the effective surface charge density caused by the immobilized probe DNA is also decreased. In the case of DNA immobilized on a diamond surface, the value of r_j is the distance between phosphate ions and the surface. If the DNA stands vertically on the diamond surface (in which case $r_j = j \times 0.2$ nm), the value of ξ is 0.23. This is the minimum value under these conditions. The ξ value becomes larger than 0.23 if the axis of the immobilized DNA is tilted through 90° (i.e., the DNA is lying on the surface).

The change in charge caused by the target DNA is described by the second term of eq 8.When the charge on the target DNA is hybridized to the probe DNA, this charge effect is screened ξ_j times according to the same argument. In addition, small counterions such as Na^+ that are present in the solution compensated for the charge associated with hybridization of target DNA. The degree of the screening effect on the charges in DNA in the electrolyte solution can be derived using Manning's counterion condensation theory,[50] according to which the fraction of counterions (θ) is 76% for the B-form of DNA, in which the average distance between phosphate pairs is 0.17 nm. Thus, the effects of charge on hybridized target DNA are screened up to 95% under our measurement conditions.

In view of the number of negative charges in the 21-mer DNA used in this experiment, $\sigma_{NH_2-probeDNA}$ can be described as $^1/_{21}\sigma_{probeDNA}$ because immobilization of one DNA molecule by an amino group through formation of an amide link eliminates one charge on the surface. Thus, the increased charge induced by hybridization ($\sigma_{targetDNA}$) is $0.4\sigma_{probeDNA}$, because the hybridization efficiency of cDNA on this surface was calculated to be 40% in our previous study.[51] Insertion of these relations into eq 8 reduces ΔV_{gs} to a function of σ_0 and $\sigma_{probeDNA}$.

To calculate the surface charge density, σ_0, we had to consider two factors for generating surface charge: ionized amino groups and hydroxyl groups. The contact-angle experiment indicated that the surface charge was almost neutralized. Therefore, we assumed that σ_0 can be estimated as 1×10^{-6} C/cm^2. In contrast, the surface charge of the aminated H-terminated diamond surface was calculated to be 3×10^{-5} C/cm^2, assuming that the amino groups on the surface are perfectly ionized. Consequently, the change in gate potential of 22 mV on the 18% aminated surface corresponds to 3×10^{-6} C/cm^2. The density of immobilized probe DNA was estimated to be 9×10^{11} cm^{-2} on this surface, given that a 21-mer is effective in its intrinsic

(50) Manning, G. S. *Macromolecules* **2001**, *34*, 4650–4655.
(51) Israelachvili, J. *Intermolecular and Surface Forces*; Academic Press: London, 1985; pp 176−181.
(52) Yang, J. H.; Song, K. S.; Kuga, S.; Kawarada, H. *Jpn. J. Appl. Phys* **2006**, *45*, L1114–L1117.

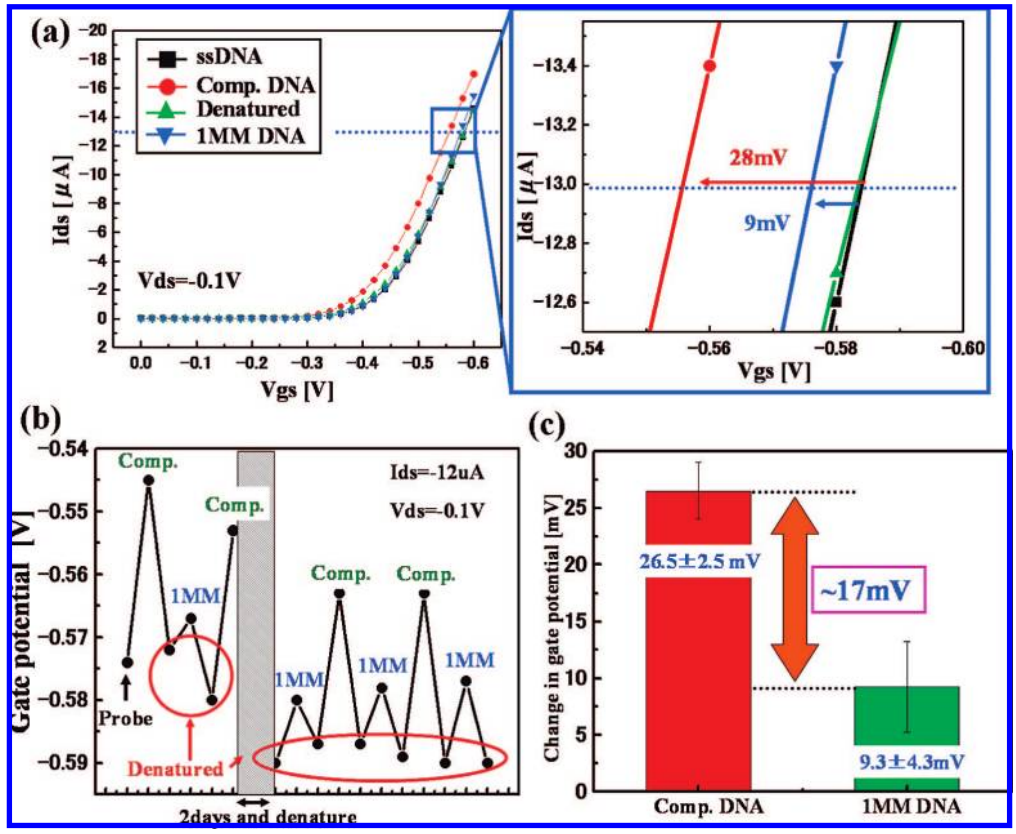

Figure 7. Static measurement for detecting singly mismatched DNA. (a) The changes in gate potential induced by hybridization of Comp. and 1MM DNAs on the partially oxidized diamond SGFET were 28 and 9 mV, respectively. (b) Detection of Comp. and 1MM DNAs was performed repeatedly on the partially oxygen-terminated SGFET. The reproducibility of detecting 1MM DNA from the differences in gate-potential shift with hybridization of target DNA was confirmed. (c) Average shifts in gate potential for the measurements in (b). The difference in the changes of gate potential for Comp. and 1MM DNAs was ~17 mV.

negative charge using this expression. However, this is the maximum value, obtained under the assumption that double-stranded DNA (ds-DNA) stands vertically on the surface. The actual density of immobilized probe DNA may be lower than this maximum estimate, because the factor ξ_j increases when DNA leans at certain angle.

Next, we applied the theory of silicon-based ISFETs to the diamond SGFET from the viewpoint of charge distribution in parallel capacitances[18] (the capacitance between the surface conductive layer of diamond and the Helmholtz plane and the capacitance of the diffusion layer), because DNA charge that affects the channel conductance exists in Debye length of the diffusion layer. This model is the same as the theory of DNA detection on an ISFET. The change in channel potential, ΔV_{gs}, can be described by:

$$\Delta V_{gs} = mN\alpha \frac{1-\theta}{C_i + C_{dif}} \tag{11}$$

where m is the fraction of DNA charge in the diffusion layer (equal to 1 in this experiment because all of the phosphate ions in DNA exist at the Debye length), N is the density of the immobilized probe molecules, α is the hybridization efficiency, θ is the fraction of DNA charge for which the condensed cations compensate, C_i on a diamond SGFET is the capacitance existing between the surface conductive layer and the Helmholtz plane, and C_{dif} is the electrical double-layer capacitance of the diffusion layer that exists between Helmholtz plane and the bulk solution. C_i exists on the diamond surface, although a SGFET does not have any passivation layer.[21,45] The estimates obtained using the typical values $C_i = 2-10\ \mu F/cm^2$ and $C_{dif} = 5-10\ \mu F/cm^2$ for diamond surface[21,45,53,54] showed that a ΔV_{gs} value of 28 mV corresponds to an immobilized probe DNA density of $7-20 \times 10^{11}\ cm^{-2}$. This value is comparable to those calculated using the Grahame equation as described above. Thus, our calculations indicate that the immobilized probe DNA density was on the order of $10^{12}\ cm^{-2}$.

Figure 6b shows the transfer characteristics of a SGFET over two hybridization/denaturation cycles. The gate voltage shifted negatively by ~22 mV in the first denaturation and positively by ~23 mV upon rehybridization of Comp. DNA. In this case, the measured shift in gate voltage was at $I_{ds} = -25\ \mu A$. This cyclical hybridization and denaturation characteristic of target DNA was also confirmed by fluorescence observations (Figure 6c). The fluorescence intensity was clearly observed with hybridization of target DNA. In contrast, this intensity was very low after denaturation. The reproducibility of the signal (gate-voltage shift by hybridization of target DNA) was determined by denaturing ds-DNA with urea solution. These results indicated that the partially functionalized SGFET is so stable that it is applicable as a reusable biosensor.

The static measurement on the SGFET was used for detection of 1MM DNA. Figure 7a shows the changes in $V_{gs}-I_{ds}$ characteristics upon hybridization of Comp. and 1MM DNAs with probe DNA. The amino-group coverage was 13% on the

(53) Dipalo, M.; Pietzka, C.; Denisenko, A.; El-Hajj, H.; Kohn, E. *Diamond Relat. Mater.* **2008**, *17*, 1241–1247.
(54) Swain, G. M.; Ramesham, R. *Anal. Chem.* **1993**, *65*, 345–351.

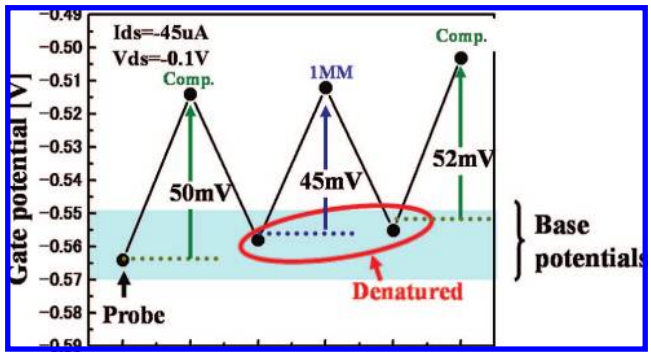

Figure 8. Static measurement for detecting singly mismatched DNA on the aminated H-terminated surface, showing the changes in gate potential induced by hybridization of Comp. and 1MM DNAs on this nonoxidized surface. The difference in the changes in gate potential for Comp. and 1MM DNAs was ~6 mV on average.

partially oxidized diamond surface. The conditions of hybridization (2× SSC buffer solution at 55 °C) and measurement (1 mM PBS at room temperature) were the same as those of the experiment to determine the denaturation characteristics. First, Comp. DNA hybridized to immobilized probe DNA, and the gate potential shifted positively by 28 mV. The gate potential returned to almost the same level upon denaturation with urea solution for 10 min. When 1MM DNA hybridized to denatured probe DNA, the gate potential shifted positively by 9 mV. This measurement was performed repeatedly to confirm the high sensitivity of detecting 1MM DNA on the partially oxidized diamond surface. Figure 7b shows the sequential shift in gate potential at $I_{ds} = -12$ μA upon hybridization. The difference between the changes in gate potential caused by hybridization of Comp. and 1MM DNAs with probe DNA immobilized on the gate surface was clearly observed in these cycles. The static characteristics of the SGFET were very stable throughout these cycles, even though the measurement was performed 2 days after the first measurement. The average changes in gate potential were 26.5 ± 2.5 mV upon hybridization of Comp. DNA and 9.3 ± 4.3 mV upon hybridization of 1MM DNA (Figure 7c). The change in gate potential caused by hybridization of Comp. DNA was ~17 mV higher than that of 1MM DNA, and the reproducibility of the high-resolution detection of mismatched DNA was confirmed by this measurement. These oscillations of gate potential by the cycling of hybridization and denaturation shown in Figure 7b indicated that this functionalized SGFET is the most promising way of detecting 1MM DNA using FET-type DNA sensors. In contrast, Figure 8 shows the same measurement performed on a SGFET aminated directly on the H-terminated surface. The gate potential shifted positively by 50 mV upon the first hybridization of Comp. DNA, returned negatively upon denaturation with urea solution, and shifted positively by 45 mV upon rehybridization of 1MM DNA. After denaturation of the 1MM DNA, Comp. DNA was rehybridized on the same H-terminated SGFET, and the gate potential changed by 52 mV. This result indicated that the difference in the change in gate potential induced by hybridization of Comp. and 1MM DNAs on the H-terminated SGFET was ~6 mV, which is much smaller than for the partially oxygen-terminated SGFET. In Figure 8, the base potentials, which are the V_{gs} values of single-stranded DNA immobilized on the channel surface, can be seen to have shifted positively, as determined by the measurement process. This corresponded to the results of our previous study using linker molecules for immobilizing DNA on H-terminated surfaces; this shift may be due to the accumulation of negative surface charges, such as halogen ions from the buffer solution during denaturation,[21] and the physisorption of nonspecific binding of target DNA on the surface. This positive shift in base potential did not occur on the partially oxidized SGFET. Our previous results also indicated that DNA physisorption onto the H-terminated surface is more pronounced than that onto the partially oxygen-terminated surface.[27]

These results indicated that the partial oxidation and direct immobilization of probe DNA on the surface without linker molecules yielded a SGFET suitable for detecting mismatched DNA because the biochemical potential changes were reflected effectively. The sensitivity of FET-based sensors is strongly related to the properties of the channel surface, such as channel mobility, capacitance on the gate surface, and threshold voltage. However, the changes in hybridization efficiency according to the surface functionalization are the main reason for the detection of the mismatched DNA with high sensitivity, because the highly sensitive detection can also be performed with fluorescence observation, the sensitivity of which is not related to the semiconducting properties of diamond.

Finally, to elucidate the hybridization kinetics, the real-time measurement was performed, and the results of calibrating the drift characteristics of the SGFET are shown in Figure 9a. In the real-time measurement, the difference between the gate-potential shifts for Comp. and 1MM DNAs was evaluated. The gate voltage of the SGFET showed a marked shift in the positive direction after injection of target DNA. Hybridization of Comp. DNA caused a shift of ~4.2 mV in V_{gs} with respect to the value at 2 min, when the target DNA was injected, and the V_{gs} shift caused by 1MM DNA was 3.2 mV when target DNA was hybridized to probe DNA for 30 min. These shifts were determined by subtracting the drift characteristic measured by injecting onto the channel surface only the 1× SSC buffer solution, which did not contain the target DNAs. With hybridization of Noncomp. DNA, the net shift from the drift characteristic of the SGFET was ~1.5 mV. The maximum difference between the signal for hybridization of Comp. DNA and that of 1MM DNA was 2 mV after ~15 min of hybridization. The difference between the hybridization kinetics for the signal on the SGFET and the results of the fluorescence observations can be attributed to the differences in temperature and ionic strength in the two measurement methods. The NaCl concentration in the buffer solution in the real-time measurement had to be higher than that in the static measurement in order to achieve sufficient hybridization efficiency to detect target DNA, and it had to be performed at room temperature because controlling the temperature of the solution on the channel surface above room temperature was difficult. In this experiment, 1× SSC buffer solution (NaCl concentration 0.15 M) was used as the measurement solution (Table 3). The change in gate potential caused by hybridization of target DNA must be small because the Debye length of this solution (~1 nm) was shorter than the length of the DNA 21-mer plus an amide bond (~9 nm).

To analyze the signal strength, we calibrated the data obtained from the real-time measurement. In this case, the shift in gate potential was caused by two factors: nonspecific binding of DNA and hybridization of target DNA. The difference between the changes in gate potential for the Comp. and Noncomp. DNAs (ΔV_{gs}^{comp}) and that for the 1MM and Noncomp. DNAs (ΔV_{gs}^{1MM}) shown in Figure 9a were due only to the hybridization of target DNA; this is true because the change in gate potential when Noncomp. DNA was injected ($\Delta V_{gs}^{physical\text{-}adsorption}$) was due to the nonspecific binding of target DNA, since the hybridization

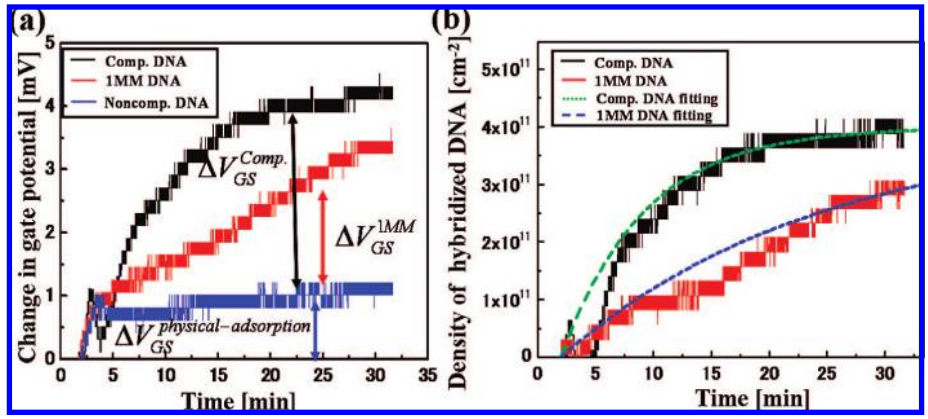

Figure 9. (a) Differential shift of V_{gs} time curves from that for the 1× SSC buffer solution. The V_{gs} time curve for the 1× SSC buffer solution indicates the drift characteristics of the SGFET. The gate-potential shift reflects the density of immobilized target DNA near the surface. (b) Density of hybridized DNA obtained by applying the Grahame equation to the data in (a). Application of the first-order Langmuir equation showed that the rate constant for 1MM DNA is a factor of 3 smaller than that for Comp. DNA.

of Noncomp. DNA with the probe DNA was minimal. The ratio of the gate-potential shift for Comp. DNA to that for 1MM DNA was 3:1 (the maximum) at 15 min, 2:1 at 20 min, and 4:3 at 30 min of hybridization. These results indicated that clarification of the signals is possible through optimization of the hybridization time and real-time measurement conditions.

To quantify the hybridization kinetics on the SGFET, we returned to the Grahame equation (eq 8). The target DNA density as a function of the change in gate potential (ΔV_{gs}^{comp} or ΔV_{gs}^{1MM}) can be calculated by applying the probe DNA density of $\sim 10^{12}$ cm^{-2}. In this analysis, we considered the coverage of oxygen termination to be 16%, which did not include the oxygen noncovalently bonded to the diamond surface, such as that in adsorbed water, because the level of oxygen termination was definitely at least 16% as determined from deconvolution of the C1s peak (Figure 2d). Figure 9b shows the calculated densities of the ds-DNA as functions of the hybridization time. The hybridization of Comp. DNA saturated at ~25 min at a density of $\sim 4 \times 10^{11}$ cm^{-2}. The hybridization reaction has been described previously:[55−57]

$$\text{probe DNA} + \text{target DNA} \xrightarrow{k} \text{ds-DNA} \qquad (12)$$

where k is the rate constant for the hybridization. Given the stability of ds-DNA, dissociation of ds-DNA is very minimal and association alone predominates. Thus, the reverse of the reaction shown in eq 12[58] is negligible.[55−57] The rate equation corresponding to eq 12 is

$$\frac{d\Gamma_{\text{ds-DNA}}}{dt} = k\Gamma_{\text{probeDNA}}[\text{target DNA}] \qquad (13)$$

As the amount of target DNA is 100 times greater than that of probe DNA and the hybridization efficiency under equilibrium conditions is 40%,[52] the decrease in target DNA density ([target DNA]) caused by hybridization with immobilized probe DNA can be neglected. Therefore, the concentration of target DNA can be considered constant (equal to the initial value [target DNA]$_0$), and the density of ds-DNA ($\Gamma_{\text{ds-DNA}}$) as a function of time is described by the first-order Langmuir equation:[59]

$$\Gamma_{\text{ds-DNA}} = \Gamma_{\text{ds-DNA}}^{\max}\{1 - \exp(-k[\text{target DNA}]_0 t)\} \qquad (14)$$

where $\Gamma_{\text{ds-DNA}}^{\max}$ is the maximum density of hybridized ds-DNA. Application of eq 14 to Figure 9b using a target DNA concentration of 100 nM yielded k values of 2×10^4 and 8×10^3 M^{-1} s^{-1} for hybridization of Comp. and 1MM DNA, respectively. Comparison of these two rate constants shows that the hybridization rate of 1MM DNA on this surface was a factor of ~3 smaller than that of Comp. DNA. Given the Debye length of the buffer solution (~1 nm), ~25% of the negative ions in DNA near the diamond surface can be detected by the SGFET. The density of physically adsorbed DNA was calculated to be 1×10^{10} cm^{-2} by applying the Grahame equation to $\Delta V_{gs}^{\text{physical-adsorption}}$ shown in Figure 9a, indicating that the nonspecific binding of DNA was about 1−2% of the hybridization of Comp. DNA.

The thermodynamic stability of ds-DNA is altered by the existence of a single base mismatch. Moreover, this study clearly showed that the difference in hybridization efficiencies due to mismatch arises because target DNAs are repelled by the negative charge resulting from oxygen termination when they approach the diamond surface. This effect is predominant only when probe DNA is immobilized very close to the diamond surface, where mismatched target DNA cannot easily hybridize with probe DNA. Through the surface negative charge, mismatched DNA can be discriminated from Comp. DNA in the harsh environment required for hybridization. In this particular immobilization method, the interaction between DNA and the diamond surface can be enhanced by the direct immobilization of DNA on the diamond surface obtained by direct surface amination of diamond.

Conclusions

The detection of mismatched DNA on a partially functionalized diamond surface was proposed. We succeeded in optical and potentiometric detection of the base mismatch of DNA using a fluorescence microscope and a SGFET, respectively. By fluorescence microscopy, differences in the signals for Comp.

(55) Tsuruoka, M.; Yano, K.; Ikebukuro, K.; Nakayama, H.; Masuda, Y.; Karube, I. *J. Biotechnol.* **1996**, *48*, 201–208.
(56) Nihira, T.; Mizuno, M.; Tonozuka, T.; Sakano, Y.; Mori, T.; Okahata, Y. *Biochemistry* **2005**, *44*, 9456–9461.
(57) Jeng, S. E.; Moll, E. A.; Roy, C. A.; Gastala, B. J.; Strano, S. M. *Nano Lett.* **2006**, *6*, 371–375.
(58) Bunimovich, L. Y.; Shin, S. Y.; Yeo, W. S.; Amori, M.; Kwang, G.; Heath, R. J. *J. Am. Chem. Soc.* **2006**, *128*, 16323–16331.
(59) Yang, G.; Wolf, K. L.; Georgiadis, R. M. *Nucleic Acids Res.* **2006**, *34*, 3370–3377.

and mismatched DNAs on aminated partially oxidized diamond surfaces were observed. Using the SGFET, the shift in the gate potential caused by the intrinsic charge of DNA was observed by evaluating static characteristics and by real-time measurement. The difference between the signals (changes in gate potential) for Comp. and 1MM DNAs was 17 mV on average, as determined by the repeated detection of these DNAs on the functionalized channel surface. This is the largest difference in gate-potential shift obtained by applying FET-type DNA sensors to detection of mismatched DNA, and the stability of functionalized the SGFET was also confirmed by the stable oscillations of gate potentials through repeated detection. The ratio of the gate-potential shift for Comp. DNA to that for 1MM DNA was 3:1 at a hybridization time of 15 min, as determined by the real-time measurement. The hybridization kinetics of 1MM DNA were ~3-fold slower than those of Comp. DNA. A surface negative charge due to oxygen termination, especially deprotonated hydroxyl groups, cancels the positive charge on partially aminated surfaces and provides a local repulsive force between immobilized DNA in the diffusion layer and the functionalized surface. Therefore, thermodynamic stability differences in hybridization affinity between complementary and mismatched DNA can be discriminated in a harsh environment for hybridization, such as repulsive force. Through the use of a SGFET, label-free potentiometric DNA sensing for detection of mismatched DNA at high resolution through control of the surface chemical bonds has been successfully demonstrated. The functionalized diamond surface provides a platform for the detection of the biochemical reaction.

Acknowledgment. This work was supported in part by a grant-in-aid from a Global Center of Excellence (GCOE) program, a Scientific Research S Grant (A07102000) from the Ministry of Education, Culture, Sports, Science and Technology, and a grant-in-aid from the Consolidated Research Institute for Advanced Science and Medical Care, Waseda University (ASMew).

Supporting Information Available: Static ($V_{ds}-I_{ds}$) curve and the leak current (I_{gs}) on a partially aminated, partially oxidized SGFET (Figure S1) and drift characteristics of functionalized SGFETs (Figure S2). This material is available free of charge via the Internet at http://pubs.acs.org.

JA710167Z